


ASCC3 promotes the immunosuppression and progression of non-small cell lung cancer by impairing the type I interferon response via CAND1-mediated ubiquitination inhibition of STAT3

Yong-Qiang Ao,^{1,2} Jian Gao,^{1,2} Chun Jin,³ Shuai Wang,^{1,2} Li-Cheng Zhang,⁴ Jie Deng,⁵ Zong-wei Chen,^{1,2} Hai-Kun Wang,⁶ Jia-Hao Jiang,^{1,2} Jian-Yong Ding ^{1,2}

To cite: Ao Y-Q, Gao J, Jin C, et al. ASCC3 promotes the immunosuppression and progression of non-small cell lung cancer by impairing the type I interferon response via CAND1-mediated ubiquitination inhibition of STAT3. *Journal for ImmunoTherapy of Cancer* 2023;**11**:e007766. doi:10.1136/jitc-2023-007766

► Additional supplemental material is published online only. To view, please visit the journal online (<http://dx.doi.org/10.1136/jitc-2023-007766>).

Y-QA, JG, CJ and SW contributed equally.

Accepted 01 November 2023



© Author(s) (or their employer(s)) 2023. Re-use permitted under CC BY-NC. No commercial re-use. See rights and permissions. Published by BMJ.

For numbered affiliations see end of article.

Correspondence to

Professor Jian-Yong Ding; ding.jianyong@zs-hospital.sh.cn

Dr Jia-Hao Jiang; jiang.jiahao@zs-hospital.sh.cn

ABSTRACT

Background Activating signal cointegrator 3 (ASCC3) has been identified as an oncogenic factor that impairs host immune defense. However, the underlying mechanisms of carcinogenesis and its impact on the antitumor immune response remain unclear. In this study, we aimed to investigate the molecular mechanisms of ASCC3 in the progression of non-small cell lung cancer (NSCLC).

Methods Single-cell sequencing data from the Gene Expression Omnibus and gene expression profiles from The Cancer Genome Atlas database were analyzed. The expression, clinical relevance and biological functions of ASCC3 in NSCLC were explored. Then, RNA sequencing, immunoprecipitation, mass spectrometry, immunofluorescence, and flow cytometry analyses were conducted to explore the underlying molecular mechanisms. In addition, in vivo experiments in mouse models were conducted to explore the probability of ASCC3 knockdown to improve the efficacy of anti-Programmed Death-1 (PD-1) therapy in NSCLC.

Results ASCC3 was significantly upregulated in NSCLC and correlated with poor pathological characteristics and prognosis in patients with NSCLC. Overexpression of ASCC3 promoted malignant phenotypes of NSCLC cells and induced an immunosuppressive tumor microenvironment, which was characterized by a decrease in CD8⁺ T cells, natural killer cells and dendritic cells but an increase in regulatory T (Treg) cells. Mechanistically, ASCC3 stabilized signal transducer and activator of transcription (STAT)3 signaling by recruiting Cullin-associated and neddylation dissociated 1 (CAND1), which inhibited ubiquitin-mediated degradation of STAT3, thereby impairing the type I interferon response of tumor cells and promoting the immunosuppression and progression of NSCLC. Furthermore, high expression of ASCC3 impaired the efficacy of anti-PD-1 therapy, and an anti-PD-1 antibody combined with ASCC3 knockdown exerted promising synergistic efficacy in a preclinical mouse model.

Conclusion ASCC3 could stabilize the STAT3 pathway via CAND1, reshaping the tumor microenvironment and inducing resistance to anti-PD-1 therapy, which promotes

WHAT IS ALREADY KNOWN ON THIS TOPIC

⇒ Numerous patients with asymptomatic non-small cell lung cancer (NSCLC) are diagnosed in advanced stages, marked by immunosuppression and disease progression. While targeted therapy and immunotherapy hold promise in NSCLC treatment, drug resistance remains a formidable challenge. Activating signal cointegrator 3 (ASCC3), identified as an oncogenic factor, may contribute to tumor progression and treatment resistance, yet its role in NSCLC remains insufficiently explored. Further investigation is warranted.

WHAT THIS STUDY ADDS

⇒ High ASCC3 expression in NSCLC cells stabilizes signal transducer and activator of transcription (STAT)3 signaling by recruiting Cullin-associated and neddylation dissociated 1 that inhibited ubiquitin-mediated degradation of STAT3, thereby impairing the type I interferon response of tumor cells and promoting the immunosuppression and progression of NSCLC. ASCC3 knockdown combined with anti-Programmed Death-1 (PD-1) therapy exerted promising synergistic efficacy in treatment of NSCLC.

HOW THIS STUDY MIGHT AFFECT RESEARCH PRACTICE OR POLICY

⇒ This study highlights the identification of ASCC3 as a potential oncogenic factor, offering a promising avenue for combination therapy with anti-PD-1 to augment NSCLC treatment efficacy and improve patient prognosis.

the progression of NSCLC. It is a reliable prognostic indicator and can be a target in combination therapy for NSCLC.

INTRODUCTION

Lung cancer is a major contributor to cancer-related deaths worldwide, with non-small cell

lung cancer (NSCLC) comprising the majority of cases.^{1,2} Many asymptomatic patients are diagnosed with NSCLC at an advanced stage, limiting the effectiveness of conventional treatments such as surgery combined with chemoradiotherapy. Somatic mutations, copy number variations, and chromosome rearrangements, including EGFR/KRAS mutations and ALK or ROS1 rearrangements,³ have been identified in NSCLC, and small molecular inhibitors targeting these genetic alterations have been developed. These drugs inhibit tumor cell proliferation and modulate the immune response, leading to improved outcomes for patients with NSCLC.⁴⁻⁶ Immunotherapy, especially immune checkpoint inhibitors, has shown promising efficacy in treating advanced NSCLC. Despite these advancements, challenges remain, including the development of resistance to various treatment options, which hampers the comprehensive management of NSCLC. Distant metastasis is a major factor contributing to the low cure and survival rates of patients with advanced NSCLC.⁷ Therefore, it is crucial to gain further insights into the mechanisms underlying NSCLC development and identify effective strategies to enhance treatment efficacy.

Previous research has demonstrated that activating signal cointegrator 3 (ASCC3) is a protein with helicase activity that is associated with DNA damage repair and immune regulation, and it might be involved in the development of several solid tumors.⁸⁻¹⁰ However, there has been no investigation into the role of ASCC3 in lung cancer. Single-cell RNA sequencing analysis has revealed differentially expressed genes in non-tumor tissues, primary tumors, and metastases of NSCLC, some of which are associated with NSCLC metastasis, by directly influencing the malignant characteristics of tumor cells or being involved in tumor progression-related signaling pathways.¹¹⁻¹³ We found that ASCC3 was also upregulated in NSCLC, and importantly, a higher expression level was observed in distant metastases. As a member of the helicase family, ASCC3 is thought to be involved in DNA damage repair and cancer progression.^{14,15} Additionally, ASCC3 has been shown to regulate the expression of immune-related genes, affecting immune cell infiltration and thyroid cancer recurrence.⁸ Through Gene Ontology (GO) and Kyoto Encyclopedia of Genes and Genomes (KEGG) analysis of our RNA sequencing data, we found that ASCC3 was involved in signal transducer and activator of transcription (STAT) signaling and type I interferon (IFN)-related pathways. Further mechanical exploration revealed that ASCC3 regulated the STAT3 signaling pathway. STAT3 is a key regulator of malignant tumor behaviors and the antitumor immune response^{16,17} and acts as a point of convergence for many oncogenic signaling pathways.^{18,19} Exploring factors that affect STAT3 expression and activation will enhance our comprehension of the intricate mechanisms underpinning tumor progression and facilitate novel therapeutic strategies.

In this study, we analyzed available gene expression profiles from the Gene Expression Omnibus (GEO) and The Cancer

Genome Atlas (TCGA) databases, revealing that ASCC3 was upregulated in NSCLC. Moreover, higher expression of ASCC3 in metastasis than in primary tumors was observed, indicating the potential role of ASCC3 in driving tumor metastasis.¹² We also demonstrated that ASCC3 might function by influencing STAT3-regulated type I IFN signaling and impairing the antitumor immune response and efficacy of anti-Programmed Death-1 (PD-1) immunotherapy. Mechanistically, ASCC3 interacts with STAT3 and recruits Cullin-associated and neddylation dissociated 1 (CAND1), which inhibits the ubiquitin (Ub)-mediated degradation of STAT3. Then, the level of phosphorylated STAT3 increased, followed by dimerization, nuclear translocation, DNA binding and transcription regulation. Consequently, STAT3 promotes the malignant features of NSCLC and inhibits the antitumor immune response by impairing the type I IFN response. Targeting ASCC3 combined with anti-PD-1 therapy may enhance the efficacy of NSCLC treatment. A deeper understanding of the mechanistic role of ASCC3 in NSCLC will contribute to the development of new therapeutic strategies.

METHODS

Data availability

To verify whether ASCC3 was involved in the progression of NSCLC, we performed data mining on available gene expression profiles from the GEO (<https://www.ncbi.nlm.nih.gov/gds/>) and TCGA (<https://xenabrowser.net/datapages/>) databases. The processed single-cell sequencing data demonstrated that the molecular and cellular reprogramming of metastatic lung adenocarcinoma was accessed from the GEO database with accession code GSE131907 (based on GPL16791 platform, *Homo sapiens*, Illumina HiSeq 2500), including 58 lung adenocarcinomas from 44 patients, which covered primary tumor, lymph node and brain metastases, pleural effusion, normal lung tissues and lymph nodes. Data were calculated and analyzed via R studio V.4.1.2 (Boston, Massachusetts, USA).

Cell culture and reagents

The human NSCLC cell lines H1299, H460, A549, H1703, and PC9 and the mouse-oriented cell line MLE-12, LLC and HEK-293T cells were purchased from the cell bank of the Chinese Academy of Sciences (Shanghai, China). These cells were cultured as previously described in Dulbecco's Modified Eagle's medium (DMEM) or Roswell Park Memorial Institute (RPMI)-1640 medium (Gibco, USA) with 10% fetal bovine serum (Invitrogen, USA), penicillin (100 IU/mL), and streptomycin sulfate (100 µg/mL) at 37°C in a thermostatic incubator containing 5% CO₂.²⁰

Vector construction and transfection

All plasmids used in this study, including flag-tagged mutant ASCC3 (deletion of domain SEC63-1 or domain C-terminal 2), were constructed by Genomeditech (Shanghai, China). The H_ASCC3-shRNA and M_AscC3-shRNA

lentiviruses were designed and purchased from Genomeditech (Shanghai, China). ASCC3-shRNA1-3 lentiviral vectors were transfected into H1299 and H460 cells, Ascc3-shRNA1-2 lentiviral vectors were transfected into LLC cells, and scramble-shRNA vectors were used as negative controls. The target sequences are shown in online supplemental table 1. The efficiency of knockdown was confirmed by western blotting and quantitative real-time PCR (qRT-PCR) after 72 hours of transfection and puromycin treatment. siRNAs against CAND1 were designed and synthesized by Genomeditech (Shanghai, China). The target sequences are shown in online supplemental table 2. The siRNA was transfected using Lipofectamine 2000 (Thermo Fisher Scientific, USA) according to the manufacturer's protocols.²⁰ The silencing efficiency was verified by western blotting and qRT-PCR analysis after 72 hours of transfection.

Patients and follow-up

A total of 173 paraffin-embedded NSCLC tissues and matched peritumoral tissues were collected from patients who underwent wedge resection, lobectomy or segmentectomy at Zhongshan Hospital, Fudan University (Shanghai, China) from 2014 to 2015 to construct a tissue microarray (TMA). Twelve pairs of frozen NSCLC and matched non-tumor tissues were randomly selected and analyzed by qRT-PCR and western blotting. All NSCLC tissues were identified by two experienced pathologists, and the clinicopathological information was collected via electronic medical records with the last follow-up information occurring in 2021. Prior to sample and information collection, informed consent was duly obtained from all participating patients.

TMA construction and immunohistochemistry staining

The construction of the TMA and immunohistochemistry (IHC) staining were performed as described previously.^{21,22} The procedures included deparaffinization with xylene, rehydration in graded ethanol (100%, 95%, 85%, and 70%) for 10 min each, quenching for endogenous peroxidase activity in 3% hydrogen peroxide, and antigen retrieval in 0.5 mM EDTA (pH 9.0) buffer by heating in boiled water for 30 min. Subsequently, the sections were cooled naturally to room temperature and incubated with the primary antibodies (online supplemental table 3) at 4°C overnight, followed by staining with horseradish peroxidase-labeled IgG (GeneTech, China). Sections were then stained with diaminobenzidine, counterstained with hematoxylin, dehydrated in ethanol, clarified in xylene, and cover-slipped. Two pathologists helped visually evaluate the scanned IHC images, and we employed a scoring system based on integral points to evaluate the density of positive staining.²² First, the cell staining intensity was scored on a scale of 0–3, with no positive staining (negative) scored as 0, light yellow staining (weakly positive) as 1, brownish-yellow staining (positive) as 2, and brown staining (strongly positive) as 3. Second, the percentage of positive cells was graded on a scale of 0–4, with $\leq 25\%$

scored as 1, 26%–50% scored as 2, 51%–75% scored as 3, and $>75\%$ scored as 4. Finally, the two scores were multiplied to obtain the final score, with a scoring range of 0–12. Then, all images were classified as high expression or low expression (cut-off=moderate intensity value 6). For the IHC results of immune cells, the molecular markers CD8, CD11c, Foxp3 and CD161 (human)/NK1.1 (mouse) represent CD8 T cells, dendritic cells, regulatory T (Treg) cells and natural killer cells, respectively.

qRT-PCR and western blotting analysis

Total RNA was obtained from both tissue samples and cultured cells by using TRIzol reagent (Invitrogen, USA), and reverse-transcribed to complementary DNA with a PrimeScript RT Reagent Kit (Takara, Japan) following the manufacturer's protocols. The cycling conditions were 95°C for 10s, 60°C for 30s, 95°C for 15s, 60°C for 60s and 95°C for 15s. Each reaction was performed in triplicate. The primer sequences for qRT-PCR are listed in online supplemental table 4. Total protein was also extracted from both tissues and cultured cells according to the manufacturer's instructions. Western blotting was performed as described previously,²³ and all the primary antibodies are listed in online supplemental table 3.

Wound-healing migration and transwell assay

The linear wound was generated by mechanically disrupting cell monolayers using a sterile 200 μ L pipette tip. The average number of migrated cells was measured by ImageJ (NIH, for Windows, USA) after taking pictures under a microscope calibrated with an ocular micrometer at a suitable time. For transwell assays, 24-well Transwell plates with 8 μ m pore size (Corning, New York, USA) were employed. A total of 50,000 cells, suspended in 200 μ L of serum-free medium, were placed in the upper chambers, with or without Matrigel (BD Biosciences, USA). Simultaneously, 200 μ L of RPMI-1640 medium containing 10% Fetal Bovine Serum (FBS) was introduced into the lower chamber. Following an appropriate incubation period, cells were fixed using 4% paraformaldehyde, stained with crystal violet, and subsequently quantified under a microscope.

Colony formation and CCK-8 assays

The colony formation assay was performed as previously described.²⁴ In brief, an initial seeding of 1,500 cells was conducted in a 6 cm culture dish, and the culture medium was replenished every 3 days for a suitable amount of time. Then, the cells were washed with phosphate-buffered saline (PBS) three times, fixed with 4% paraformaldehyde for 15 min, and stained with 0.4% crystal violet for 15 min. Afterward, the stained colonies were imaged and counted by ImageJ (NIH, for Windows, USA) and averaged over duplicate wells. Cell proliferation was evaluated by the Cell Counting Kit-8 (CCK-8, Yeasen, Shanghai, China) and performed as described previously.²⁵ Briefly, cells were seeded in 96-well plates (1,000 cells per well) and incubated

overnight. Then, 10 μ L of CCK-8 reagent was added to each well for 2 hours every day before detection for 5 days. The absorbance was determined at a wavelength of 450 nm.

In vivo tumor growth

Male BALB/c nude mice aged 4–5 weeks were purchased from GemPharmatech (Jiangsu, China), and male C57BL/6 mice aged 4–5 weeks were purchased from Jiesijie (Shanghai, China). All mice were maintained in accordance with the established principles of the three Rs (replacement, reduction, and refinement) in the Center of Experimental Animals of Zhongshan Hospital, Fudan University. The animal experiments were approved by the Animal Experimentation Ethics Committee of Zhongshan Hospital (approval No. DSF-2021-072). For in vivo tumor growth, approximately 5×10^6 cells were resuspended in 100 μ L DMEM complete medium and subcutaneously injected into the right flanks of the nude mice. The tumor size was assessed and recorded every 3 days, and when the tumor size reached 1.5 cm, all mice were sacrificed. The entire subcutaneous tumors were resected, some of which were used for tumor immune microenvironment investigation via flow cytometry, while the others were fixed with 4% paraformaldehyde and embedded in paraffin for further IHC analysis.

Flow cytometry and immunofluorescence assays

Flow cytometry analysis was performed as described in a previous study²⁶ to investigate the immune cell profiles of subcutaneous tumors and to detect the apoptotic ratio of cultured cells. Fresh tumor tissues were homogenized into single-cell suspensions, and immune cells were isolated with Percoll. Then, they were washed with PBS, vortexed and stained with antibodies (online supplemental table 3) against cell-surface molecules for 30 min at 4°C. Staining buffer (PBS with 1% FBS and 0.2% EDTA) was added to wash the samples by vortexing and centrifugation (350g, 4°C, 6 min) for further analysis. A total of 10^5 cultured cells were suspended in a 15 mL tube, washed with PBS and stained with annexin V and PI (Yeasen, Shanghai, China). All positively stained cells were counted by BD FACS Fortessa (Beckman Coulter, Brea, California, USA), and the data were analyzed using FlowJo software V.10 (Treestar, San Carlos, California, USA). Immunofluorescence was performed as previously described²⁷ to detect the location and expression of target proteins. Briefly, prepared cell slides were fixed with 4% paraformaldehyde, incubated in 0.3% Triton X-100, blocked with 5% FBS, washed with PBS and then stained with primary antibodies (online supplemental table 3) at 4°C overnight. Then, the cell slides were incubated with the appropriate secondary antibody, and the nuclei were counterstained with 4',6-diamidino-2-phenylindole (DAPI, Yeasen, Shanghai, China). The fluorescence intensity

was evaluated by confocal laser scanning microscopy (LSM510, Zeiss, Germany).

Immunoprecipitation assay and Co-IP combined with mass spectrometry

Cells were harvested in immunoprecipitation (IP) lysis buffer with protease inhibitor and rocked for 30 min on ice. Then, the insoluble material was removed by 12,000 \times g centrifugation, and precleared cell lysates with total protein were incubated with a primary antibody (online supplemental table 3) on a rocker overnight at 4°C. Then, protein A-Sepharose and G-Sepharose beads (MedChem-Express, USA) were added to the IP mixture for 3 hours. The precipitates were washed with PBS three times, and then the target protein was eluted from the magnetic beads. Next, the immunoprecipitants were detected by a silver staining kit (Solarbio, Beijing, China), and a mass spectrometry (MS) assay was performed to detect the potential candidates. IP and MS were performed in H1299 and H460 cells, and subsequent western blotting was performed with the target antibody as previously described.²³

Ubiquitination assay

H1299/H460-shASCC3/shNC cells were transiently transfected with hemagglutinin (HA)-tagged Ub vectors with or without administration of 10 μ M MG-132 (Selleck, Texas, USA). After a 48-hour incubation period, the cells were rinsed with PBS and exposed to 10 μ M MG-132 for 8 hours. Subsequently, cell lysis was performed, followed by IP using anti-CAND1 and anti-STAT3 antibodies. The ubiquitination of target proteins was assessed via sodium dodecyl sulfate-polyacrylamide gel electrophoresis (SDS-PAGE) after immunoblotting with an anti-HA antibody.

Statistical analysis

The experiments were independently repeated two to five times. All data were analyzed using SPSS V.23.0 (Chicago, Illinois, USA) and Prism V.9.0 software (GraphPad) and are shown as the mean values \pm SD. Unpaired Student's t-tests were employed to assess distinctions between two groups, while χ^2 tests were used for comparing categorical variables. Spearman correlation analysis was conducted to explore correlations between the levels of ASCC3, CAND1, STAT3, CD8, NK1.1 (CD161), CD11C, Foxp3, STAT3, ISG15 and IRF7. The Kaplan-Meier and log-rank tests were applied to assess prognostic variances in patients with NSCLC, while Cox's regression model was employed to explore factors with independent prognostic significance. All p values were two tailed, and statistical significance was defined as $p < 0.05$.

RESULTS

ASCC3 is upregulated in NSCLC and correlated with worse clinicopathological characteristics and patient prognosis

To reveal the role of ASCC3 in NSCLC, we analyzed available single-cell sequencing data (accessed by GSE131907)

and the TCGA database (<https://xenabrowser.net/datapages/>). The results consistently demonstrated upregulation of ASCC3 in NSCLC across both data sets (figure 1A,B). Additionally, we compared ASCC3 expression levels in primary tumors and various metastatic sites, revealing significantly higher expression in brain and lymphoid metastases (figure 1C). To further validate this finding, we conducted western blotting and qRT-PCR in 12 paired tumor and peritumor tissues. The results indicated significantly higher levels of ASCC3 at both the protein and messenger RNA (mRNA) levels in NSCLC tissues than in peritumor tissues (figure 1D,E). In addition, IHC staining and quantification analysis of the TMA showed that the expression of ASCC3 was upregulated in NSCLC tissues compared with peritumor tissues, and the ASCC3 protein was predominantly localized in the cytoplasm of cancer cells (figure 1F). Moreover, in patients with lymph node metastasis, we observed an even higher ASCC3 expression level in primary tumors than in those without lymph node metastasis (figure 1G,H). The relationship between ASCC3 expression and clinicopathological characteristics is summarized in table 1. These results indicated that high expression of ASCC3 was correlated with larger tumor size, higher Programmed Death Ligand-1 (PD-L1) expression, advanced tumor stage and lymph node metastasis (figure 1I–L). Univariate and multivariate analyses demonstrated that, apart from tumor stage and lymph node metastasis, the ASCC3 expression level independently predicted the overall survival (OS) and recurrence-free survival (RFS) of patients with NSCLC (online additional file 1 and figure 1M,N). Additionally, Kaplan-Meier analysis revealed that patients with high ASCC3 expression had lower OS and RFS rates than those with low ASCC3 expression (figure 1O,P). These results were further corroborated by a larger cohort analysis from the TCGA database, showing that high ASCC3 expression (using a cut-off of the median expression value of 2.62) correlated with a worse probability of OS (online supplemental figure 1A).

High ASCC3 expression promotes the progression of NSCLC both in vitro and in vivo

We also tested the expression of ASCC3 in some NSCLC cell lines and confirmed higher expression in some cell lines than in the normal cell line Human Bronchial Epithelial cell (HBE) (figure 2A). H1299 and H460 cells with the highest expression level of ASCC3 were transfected with an ASCC3-shRNA lentivirus. Following the validation of transfection efficiency (figure 2B,C), two stably transfected cell lines were generated with shRNA selected for the subsequent experiments (referred to as shASCC3 vs shNC). Colony formation and CCK8 assays demonstrated that ASCC3 knockout inhibited the proliferation of NSCLC cells (figure 2D–G). Wound healing and Transwell assays exhibited significant inhibitory effects on the migration of ASCC3 knockdown cells (figure 2H–M). Similarly, the Matrigel Transwell assay revealed that ASCC3 knockdown impaired the invasion

of both H1299 and H460 cells (figure 2N,O). Moreover, in vivo assays of nude mice subcutaneously implanted with H1299-shNC/shASCC3 cells (figure 2P) showed that the expression of ASCC3 was significantly downregulated in shASCC3 subcutaneous tumors compared with that in shNC tumors (figure 2Q), and ASCC3 knockdown inhibited the growth of NSCLC (figure 2R). Overall, these results revealed that ASCC3 promoted the progression of NSCLC and that ASCC3 knockdown could inhibit this process.

ASCC3 is involved in type I interferon signaling and reshapes the tumor microenvironment

To investigate the potential mechanisms by which ASCC3 promotes NSCLC progression, we conducted RNA sequencing using H1299-shASCC3/shNC cells. A total of 480 genes were identified as significantly upregulated or downregulated, with 137 genes upregulated (log₂-fold change value ≥ 1), 278 genes downregulated (log₂-fold change value < 1) and 65 genes stable (log₂-fold change value between -1 and 1) (figure 3A and online supplemental figure 1B). GO and KEGG analyses revealed that ASCC3 was closely associated with immune response regulation and involved in several important pathways, including type I IFN signaling (figure 3B,C). Furthermore, several type I IFN-stimulated genes, such as ISG15, IFIT1, and CXCL10, were upregulated in the ASCC3 knockdown group (figure 3A). To further explore these findings, we performed gene set enrichment analysis using all detected upregulated or downregulated genes. The results confirmed a positive correlation between ASCC3 knockdown and the immune response as well as type I IFN signaling (figure 3D,E). Conversely, ASCC3 knockdown showed a negative correlation with Janus Kinase (JAK)/STAT3 signaling (figure 3F). Based on current knowledge of cancer-related signaling pathways, it was hypothesized that ASCC3 might play a role in reshaping the tumor microenvironment (TME) of NSCLC through type I IFN signaling. To verify this hypothesis, we conducted IHC staining of immune cells on the TMA. The results showed a significant decrease in the infiltration of CD8⁺ T cells, dendritic cells (DCs), and natural killer (NK) cells, while Treg cells increased in the ASCC3^{high} group (figure 3G,H). In addition, we confirmed that ASCC3 was highly expressed in the mouse-derived cell line Lewis lung carcinoma (LLC) compared with the mouse-derived normal lung epithelial cell line MLE-12 (online supplemental figure 1C). Then, LLC-shAscc3/shNC cells were constructed and subcutaneously implanted into C57BL/6 mice, demonstrating that Ascc3 knockdown inhibited tumor growth (online supplemental figure 1D,E). Subcutaneous tumors were obtained for further flow cytometry and IHC analysis. Immune profiles were detected via flow cytometry, and the results revealed that, compared with LLC-shNC cells, CD8⁺ T cells, NK cells and DCs increased but Treg cells decreased in tumors derived from LLC-shAscc3 cells (figure 3I,J). IHC staining of CD8⁺ T cells, NK1.1⁺ NK cells, CD11C⁺ DCs and Foxp3⁺ Treg cells in the

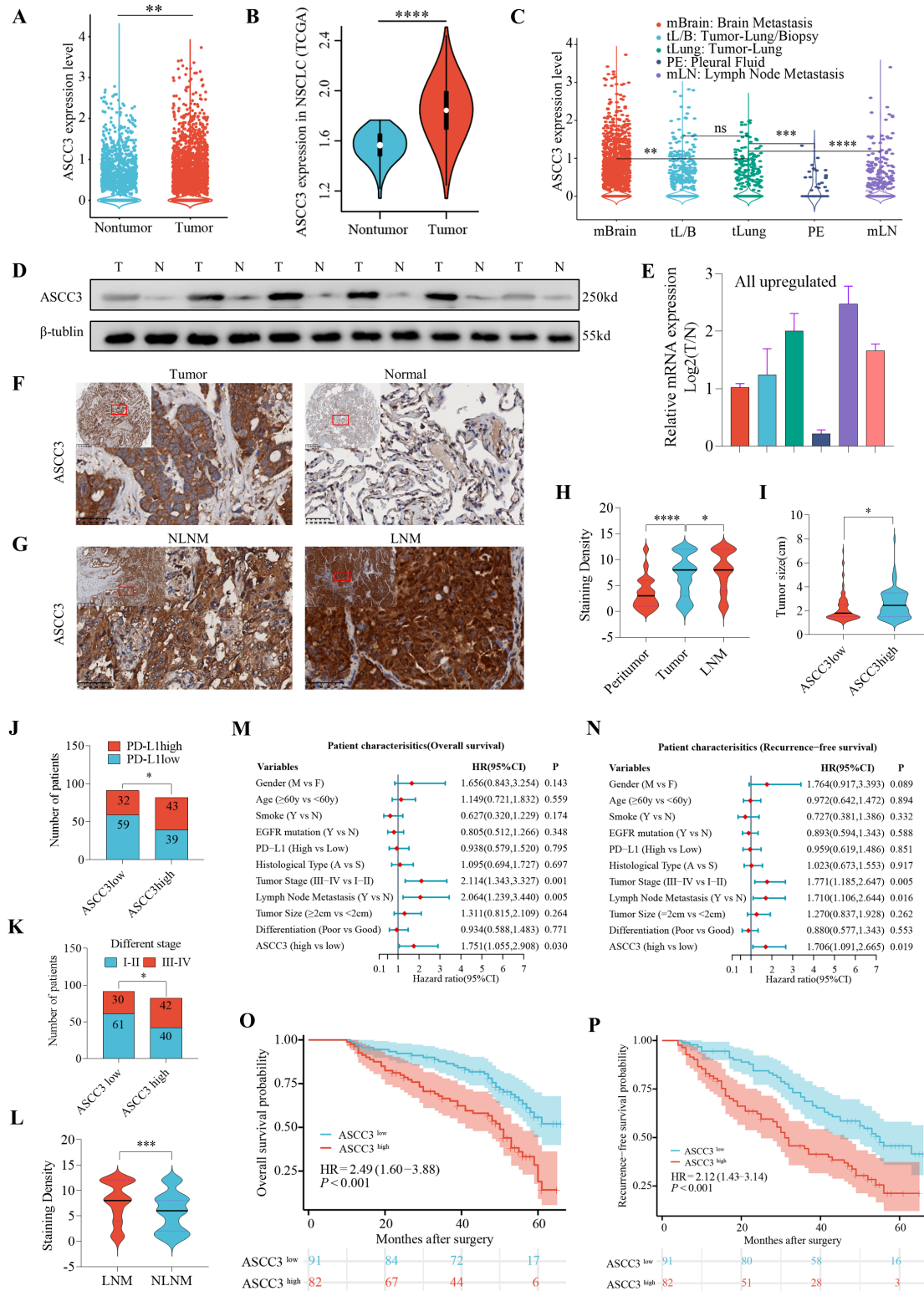


Figure 1 ASCC3 is upregulated in NSCLC and correlated with worse clinicopathological characteristics and patient prognosis. (A–C) ASCC3 was upregulated in NSCLC, especially in metastatic foci. (D–F) Expression of ASCC3 was higher in NSCLC tissues than in peritumor tissues at both the protein and mRNA levels. (G,H) ASCC3 expression was higher in tumors with lymph node metastasis (LNM) than in those with no lymph node metastasis (NLNM). (I–L) High expression of ACC3 was correlated with larger tumor size, higher PD-L1 expression, advanced tumor stage and lymph node metastasis. (M,N) Tumor stage, lymph node metastasis and ASCC3 expression level were independent risk factors for the overall survival (OS) and recurrence-free survival (RFS) of patients with NSCLC. (O,P) Patients with high ASCC3 expression had lower OS and RFS than those with low ASCC3 expression. *p < 0.05, **p < 0.01, ***p < 0.001, ****p < 0.0001, ns: not significant. TCGA, The Cancer Genome Atlas; PD-L1, Programmed Death Ligand-1; ASCC3, activating signal cointegrator 3; mRNA, messenger RNA; NSCLC, non-small cell lung cancer.

Table 1 Correlations between ASCC3 and clinicopathological features in 173 patients with non-small cell lung cancer

Characteristics	Number of patients		P value
	ASCC3 ^{low}	ASCC3 ^{high}	
Age (years)			
Mean±SD	57.7±8.8		
<60	44	46	0.309
≥60	47	36	
Gender			
Female	46	38	0.580
Male	45	44	
Smoke			
Yes	39	38	0.645
No	52	44	
EGFR mutation			
Yes	51	43	0.635
No	40	39	
PD-L1			
High	32	43	0.022 (*)
Low	59	39	
Tumor size (cm)			
Mean±SD	2.71±1.19		
≥2	39	55	0.001 (**)
<2	52	27	
Pathological stage			
I-II	61	42	0.034 (*)
III-IV	30	40	
Lymph node metastasis			
Yes	37	57	0.000 (****)
No	54	25	
Histological type			
Adeno-	53	40	0.213
Squamous-	38	42	
Differentiation			
Good	55	48	0.799
Poor	36	34	

PD-L1: Programmed Death Ligand-1.
ASCC3, activating signal cointegrator 3.

tumor tissues also exhibited a similar trend (figure 3K,L). To further validate these results, we conducted an analysis of tumor immune infiltration (CIBERSORT) using the TCGA database. NSCLC samples were divided into ASCC3^{high} and ASCC3^{low} groups (cut-off=median expression value of 2.62), and differences in immune cell infiltration were analyzed. Compared with those of the ASCC3^{low} group, plasma cells, activated CD8⁺/CD4⁺ T cells, NK cells, type I macrophages and DCs significantly

decreased, while Treg cells increased in the ASCC3^{high} group (online supplemental figure 1F), confirming the obtained results. These findings led to the hypothesis that ASCC3 is involved in type I IFN signaling and promotes the progression of NSCLC to some degree by limiting antitumor immunity.

ASCC3 interacts with STAT3 and modulates its protein level

We further investigated the molecular mechanisms by which ASCC3 influenced the TME of NSCLC. IP assays were performed in H1299 and H460 cells using an ASCC3 antibody. MS analysis of IP protein suspension samples from both cell lines revealed 28 potential proteins that could interact with ASCC3, and the top 10 were listed (figure 4A,B), including STAT3. Given that STAT3 could influence IFN signaling and KEGG, Gene Set Enrichment Analysis (GSEA) of our sequencing data indicated that ASCC3 could also influence JAK/STAT3 signaling (figure 3C,F). We aimed to explore the connection between ASCC3 and STAT3. Moreover, IP assays were conducted, followed by silver staining (figure 4C). We found that ASCC3 could pull down STAT3, which was further verified by a Co-Immunoprecipitation (Co-IP) assay in both H1299 and H460 cells (figure 4D). Additionally, Immunofluorescence (IF) analysis further confirmed the colocalization of ASCC3 and STAT3 in the cytoplasm of both H1299 and H460 cells (figure 4E,F). To explore the possibility of mutual regulation between ASCC3 and STAT3, we detected the expression of STAT3 at both the transcriptional and translational levels in H1299-shASCC3 cells. The results showed that knockdown of ASCC3 decreased the protein level but not the mRNA level of STAT3 (figure 4G,H). ASCC3 contains six domains that are responsible for the interaction with other molecules, such as ATP and ASCC1.^{28 29} To identify the exact domain of ASCC3 that interacts with STAT3, we constructed six flag-tagged vectors encoding these fragments of ASCC3 (figure 4I and online supplemental figure 2A–F). We transfected these vectors into H1299 cells, and a Co-IP assay showed that domain 3 (SEC63-1) of ASCC3 was primarily responsible for the interaction with STAT3 (figure 4J). To explore whether ASCC3 influenced the protein level of STAT3 by regulating its ubiquitination level, we constructed a flag-tagged mutant ASCC3 with deletion of SEC63-1 (online supplemental figure 2G) and transfected it into H1299 cells. IP assays confirmed that knockdown of ASCC3 and mutant ASCC3 increased the ubiquitination level of STAT3 (figure 4K), which might be responsible for the decrease in STAT3 protein levels.

ASCC3 recruits CAND1 to stabilize STAT3 in NSCLC

Since no evidence indicated that ASCC3 could directly regulate protein levels, previous studies have demonstrated the role of ASCC3 in the process of functional protein complex assembly.^{10 30 31} We speculated that ASCC3 regulated STAT3 protein levels by recruiting other molecules. Of the top 10 proteins that could

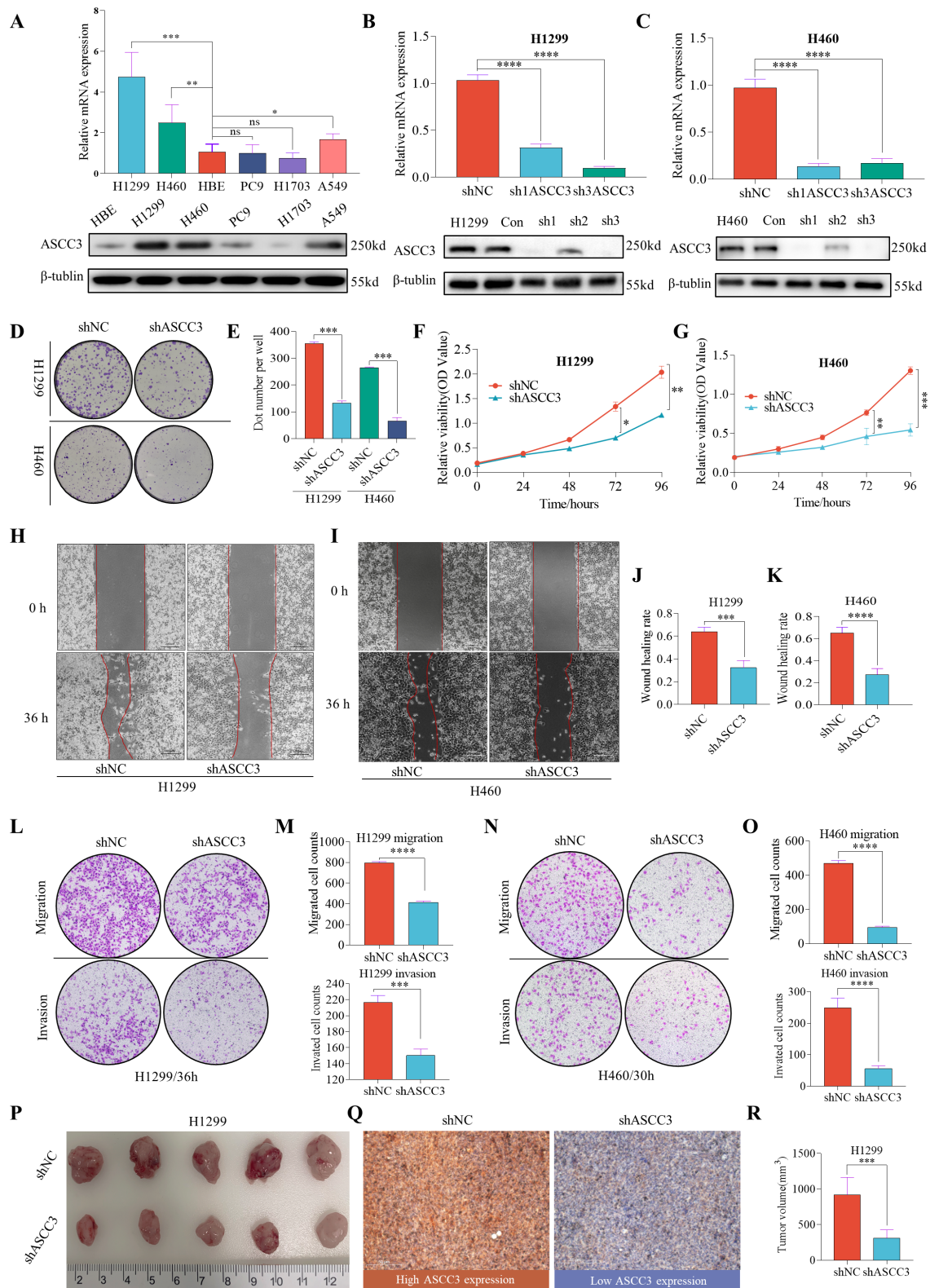


Figure 2 High ASCC3 expression promotes NSCLC progression both in vitro and in vivo. (A) ASCC3 was also highly expressed in some NSCLC cell lines compared with the normal cell line HBE. (B, C) ASCC3-shRNA lentivirus was transfected into H1299 and H460 cells (with the highest expression level of ASCC3), and the transfection efficiency was validated. (D–O) The colony formation, Cell Counting Kit-8, wound healing and (non)Matrigel Transwell assays revealed that ASCC3 knockdown inhibited the proliferation, migration and invasion capability of NSCLC cells. (P) In vivo assays of nude mice subcutaneously implanted with H1299-shNC/shASCC3 cells. The expression of ASCC3 significantly decreased in shASCC3 subcutaneous tumors compared with that in the shNC group (Q) and ASCC3 knockdown inhibited the growth of NSCLC (R). * $p < 0.05$, ** $p < 0.01$, *** $p < 0.001$, **** $p < 0.0001$, ns: not significant. HBE, human bronchial epithelial cell; ASCC3, activating signal cointegrator 3; mRNA, messenger RNA; NSCLC, non-small cell lung cancer.

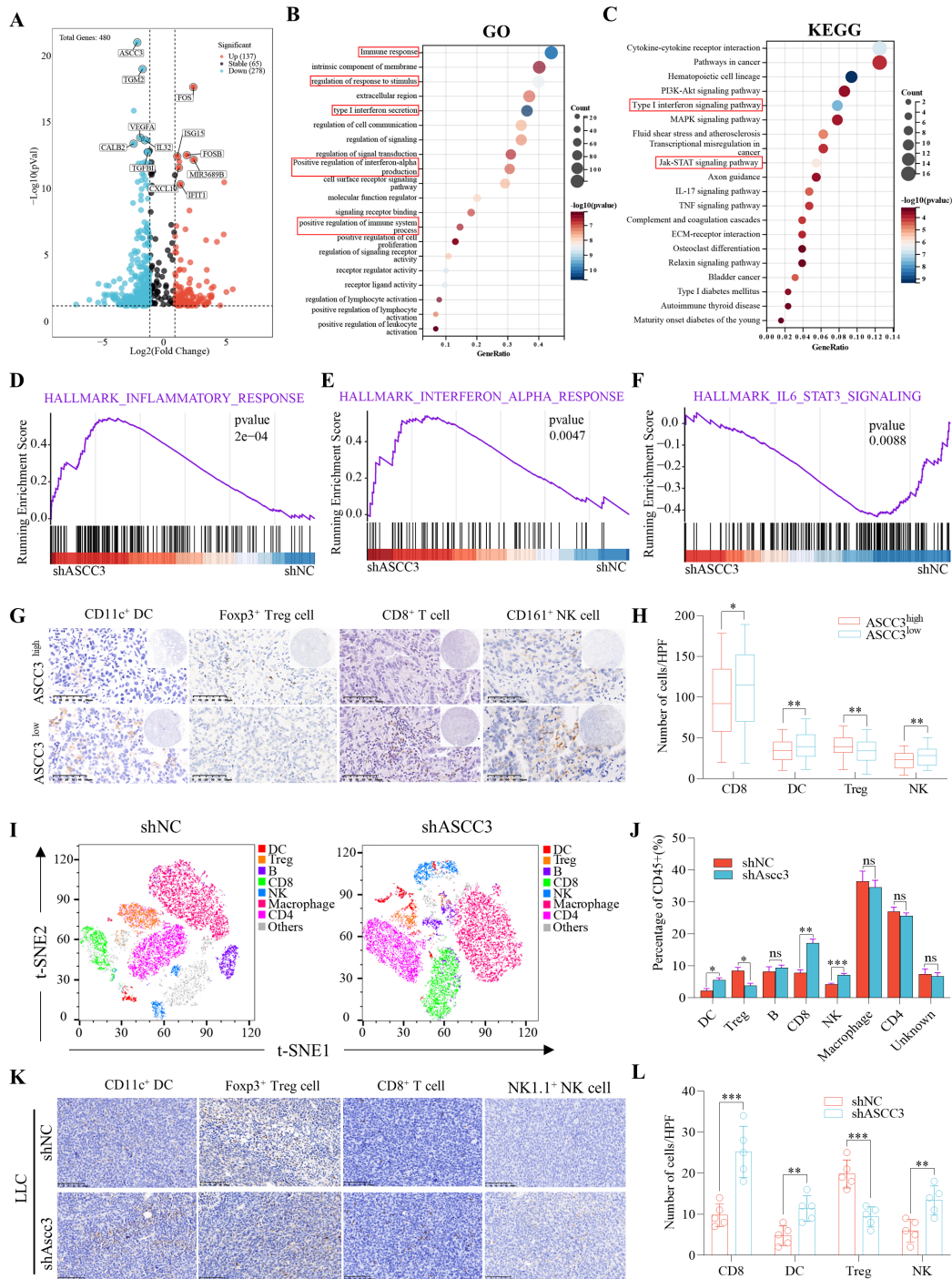


Figure 3 ASCC3 is involved in type I interferon signaling and reshapes the tumor microenvironment. RNA sequencing of H1299-shASCC3/shNC cells detected 480 significantly downregulated or upregulated genes. (B,C) GO and KEGG analyses revealed that ASCC3 was closely associated with immune response regulation and involved in several important pathways, including type I interferon signaling. (D–F) Gene set enrichment analysis of all upregulated or downregulated genes confirmed that knockdown of ASCC3 was positively correlated with the immune response and type I interferon signaling but negatively correlated with JAK/STAT3 signaling. (G,H) IHC staining of immune cells on the tissue microarray showed a significant decrease in the infiltration of CD8⁺ T cells, dendritic cells (DCs), and natural killer (NK) cells, while Treg cells increased in the ASCC3^{high} group. (I,J) Immune profiles of subcutaneous tumors derived from LLC cells were detected via flow cytometry and revealed that, compared with LLC-shNC cells, CD8⁺ T cells, NK cells and DCs increased but Treg cells decreased in tumors derived from LLC-shASCC3 cells. (K,L) IHC staining of CD8⁺ T cells, NK1.1⁺ NK cells, CD11c⁺ DCs and Foxp3⁺ Treg cells in the tumor tissues also showed a similar trend. * $p < 0.05$, ** $p < 0.01$, *** $p < 0.001$, **** $p < 0.0001$, ns: not significant. GO, Gene Ontology; KEGG, Kyoto Encyclopedia of Genes and Genomes; MAPK, mitogen-activated protein kinase; JAK, janus kinase; TNF, tumor necrosis factor; ECM, extracellular matrix; ASCC3, activating signal cointegrator 3; Treg, regulatory T cells; t-SNE, t-distributed Stochastic Neighbor Embedding; IHC, immunohistochemistry; HPF, high power field; LLC, Lewis lung carcinoma; NSCLC, non-small cell lung cancer; STAT3, signal transducer and activator of transcription.

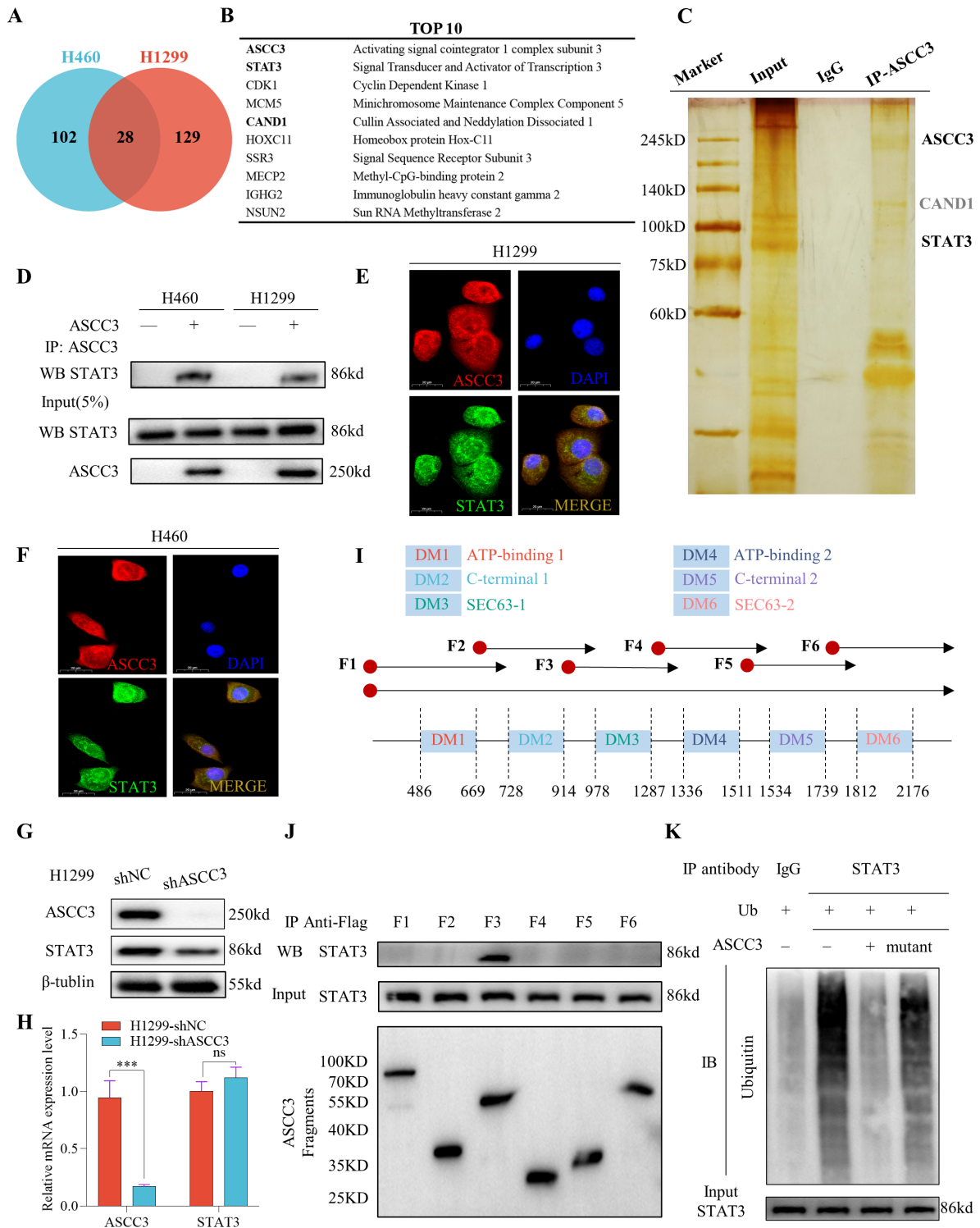


Figure 4 ASCC3 interacts with STAT3 and modulates its protein level. (A, B) Mass spectrometry analysis of IP protein (with ASCC3 antibody) in H1299 and H460 cells revealed 28 potential proteins that could interact with ASCC3, and the top 10 are listed. (C, D) Polyacrylamide gel electrophoresis of IP samples was conducted, and silver staining of the gel showed that ASCC3 could pull down STAT3, which was further verified by western blotting of IP samples from both H1299 and H460 cells. (E, F) IF analysis confirmed the colocalization of ASCC3 and STAT3 in both H1299 and H460 cells. (G, H) Knockdown of ASCC3 decreased the protein level but not the mRNA level of STAT3. (I) Vectors encoding six fragments of ASCC3 containing six potential binding domains with other molecules were transfected into H1299 cells. (J) Co-IP assays confirmed that domain 3 (SEC63-1) of ASCC3 was mainly responsible for binding with STAT3. (K) IP combined with ubiquitination assay confirmed that knockdown of ASCC3 and mutant ASCC3 (deletion in SEC63-1) increased the ubiquitination level of STAT3. *** $p < 0.001$, ns: not significant. Co-IP, Co-Immunoprecipitation; WB, Western blotting; IF, Immunofluorescence; ASCC3, activating signal cointegrator 3; CAND1, Cullin-associated and neddylation dissociated 1; IP, immunoprecipitation; mRNA, messenger RNA; STAT3, signal transducer and activator of transcription; Ub, ubiquitin.

interact with ASCC3, CAND1, a molecule that regulates Cullin-RING Ub ligases, might play a role in stabilizing STAT3 by inhibiting its ubiquitination. We found that CAND1 was also upregulated in NSCLC, especially in the metastatic foci (online supplemental figure 3A–F), and was correlated with immunosuppression and poor prognosis of patients with NSCLC (online supplemental figure 3I,J). In addition, we conducted IP assays in H1299 cells with an anti-ASCC3 antibody, and silver staining on PAGE gels showed that ASCC3 could pull down CAND1 and STAT3 (online supplemental figure 4A), supporting our previous results (figure 4C). As a reverse verification, we found that CAND1 could also pull down ASCC3 and STAT3 (figure 5A). Co-IP assays confirmed that the interaction of ASCC3 with CAND1 and domain 5 of ASCC3 (C-terminal 2) was responsible for their binding (figure 4I and figure 5B,C). Then, we verified that both STAT3 and CAND1 were located in the cytoplasm of H1299 and H460 cells. (figure 5D,E). Moreover, we constructed a flag-tagged mutant ASCC3 with deletion of C-terminal 2 (online supplemental figure 2H) and transfected it into H1299 cells, and we found that ASCC3 mutation impaired the interaction of CAND1 and STAT3 (figure 5F). In H1299-^{ASCC3 mutant} cells, we also observed that the expression of STAT3 was downregulated and that the colocalization of CAND1 and STAT3 decreased (figure 5G). These findings suggested that ASCC3 might act as a scaffold and interact with both CAND1 and STAT3. Then, we interfered with CAND1 expression in H1299 and H460 cells (siCAND1) to explore the mutual regulation between CAND1 and STAT3 (online supplemental figure 3G,H). The results showed that siCAND1 decreased the protein level but did not influence the transcription of STAT3 (figure 5H,I). To further confirm whether CAND1 regulates the protein level of STAT3 by inhibiting its ubiquitination, we conducted an IP assay. H1299/H460-^{ASCC3 mutant}/ASCC3 cells (siCAND1 or not) were transiently transfected with HA-tagged Ub vectors, and ubiquitination of targeted proteins was analyzed after immunoblotting with an anti-HA antibody. The results showed that mutation of ASCC3 or interference of CAND1 upregulated the ubiquitination level of STAT3. Moreover, in ASCC3-CAND1 cells, the ubiquitination level of STAT3 was similar to that in ASCC3-siCAND1 cells that were administered the ubiquitination inhibitor MG-132 (10 μ M, 48 hours) (figure 5J). Collectively, these findings indicated that ASCC3 recruited CAND1 to STAT3 and that CAND1 upregulated the protein level of STAT3 by inhibiting the Ub-mediated degradation of STAT3.

ASCC3 stabilizes STAT3 signaling to inhibit the type I IFN response

We previously demonstrated that high expression of ASCC3 decreased the infiltration of CD8⁺ T, DC and NK cells while increasing Treg cells. Based on the finding that ASCC3 can stabilize STAT3 and influence its protein level through CAND1, we hypothesized that ASCC3 was involved in shaping the TME via STAT3 signaling.

Accumulating evidence has revealed that STAT3 hyperactivation mediates tumor-induced immunosuppression,^{32,33} with one of the mechanisms being its negative regulatory role in IFN-related signaling pathways. Through analysis of sequencing data, we also found that ASCC3 was associated with type I IFN secretion and type I IFN signaling (figure 3B,C,E). Moreover, type I IFN-stimulated genes were significantly upregulated in H1299-shASCC3 cells, while genes that negatively regulate type I IFN signaling were downregulated (figure 6A). Knockdown of ASCC3 or CAND1 impaired the activation of JAK/STAT3 signaling by IFN- α and led to the upregulation of several important type I IFN-stimulated genes, such as IRF7, IFIT1 and ISG15, at both the transcriptional and translational levels (figure 6B–F) (IFN- α used in this study is listed in online supplemental table 5). The proliferation of the H1299-shASCC3 cells was significantly impaired, while apoptosis was markedly enhanced compared with that of the shNC group after stimulation with IFN- α (5 ng/mL) (figure 6G–I). To determine the role of ASCC3 in regulating the type I IFN response, we explored the expression correlation of ASCC3 with CAND1 and several IFN- α -stimulated genes in the TCGA database. The results suggested a positive correlation between the expression of STAT3 and ASCC3, while the expression of IFN- α -stimulated genes such as IRF7 and ISG15 was negatively correlated with ASCC3 expression (figure 6J). We also tested the expression of ASCC3, STAT3 and these IFN- α -stimulated genes via IHC staining in an NSCLC TMA to verify the findings in TCGA data analysis, and the results showed a similar trend (figure 6K,L). Overall, these results indicated that ASCC3 impaired the type I IFN response of tumor cells via CAND1 and STAT3 signaling, which induced a suppressive TME in NSCLC.

ASCC3 impairs the efficacy of PD-1 blockade, and knockdown of ASCC3 sensitizes NSCLC to anti-PD-1 treatment

Considering that type I IFN can potentiate anti-PD-1 therapy in tumor treatment,^{34,35} we hypothesized that ASCC3 might hinder the immune response and the efficacy of anti-PD-1 therapy in NSCLC. To confirm this in vivo, we first conducted IP assays, which showed that ASCC3 could pull down both CAND1 and STAT3 in LLC cells (online supplemental figure 4B,C). Then, we constructed LLC-siCand1 cells (online supplemental figure 4D,E). We found that IRF7, IFIT1 and ISG15 were upregulated in LLC-shAscc3 cells and LLC-siCand1 cells compared with normal control cells at both the translational and transcriptional levels (online supplemental figure 4F–I). In addition, IFN- α stimulation activated JAK/STAT3 signaling in LLC cells (online supplemental figure 4J). This finding indicated that in vivo experiments in mice could simulate molecular and cellular changes in humans. Subsequently, we investigated the potential effects of ASCC3 on the efficacy of anti-PD-1 therapy in C57BL/6 mice bearing LLC-shAscc3 and LLC-shNC tumors. Anti-PD-1 or IgG was administered

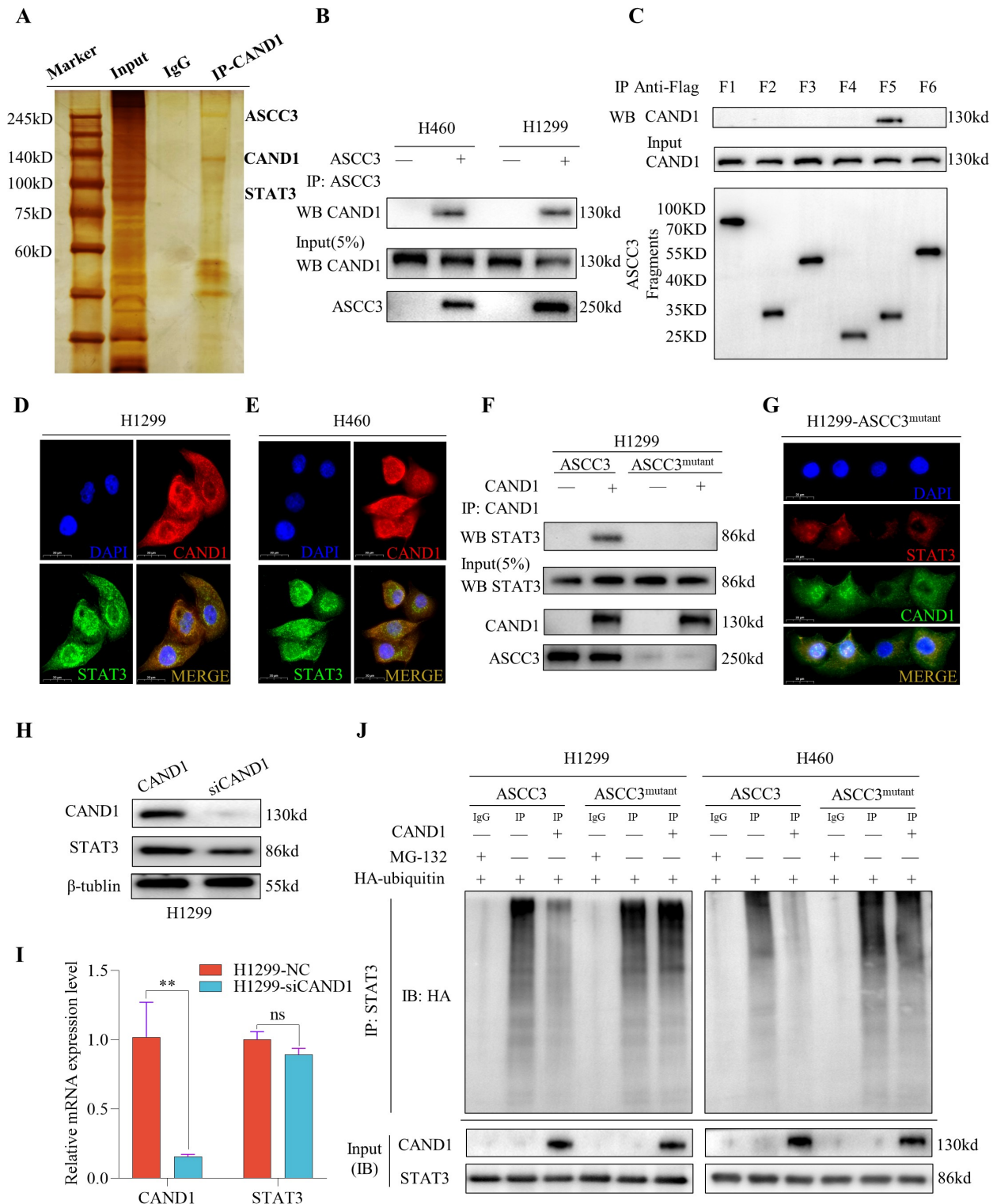


Figure 5 ASCC3 recruits CAND1 to stabilize STAT3 in NSCLC. (A) CAND1 could pull down ASCC3 and STAT3. (B,C) Co-IP assay confirmed that the interaction of ASCC3 with CAND1 and domain 5 of ASCC3 (C-terminal 2) was responsible for their binding. (D,E) IF assay in both H1299 and H460 cells showed colocalization of CAND1 and STAT3. (F) ASCC3 mutation (deletion in the C-terminal 2) impaired the interaction of CAND1 and STAT3. (G) In H1299-ASCC3^{mutant} cells, the expression of STAT3 was downregulated, and the colocalization of CAND1 and STAT3 decreased. (H,I) Interference with CAND1 decreased the protein level but did not influence the transcription of STAT3. (J) Mutation of ASCC3 or interference of CAND1 upregulated the ubiquitination level of STAT3, and in ASCC3-CAND1 cells, the ubiquitination level of STAT3 was similar to that of ASCC3-siCAND1 cells that were administered the ubiquitination proteasome inhibitor MG-132 (10 μM, 48 hours) as IgG control. **p<0.01, ns: not significant. Co-IP, co-immunoprecipitation; WB, Western blotting; IF, immunofluorescence; ASCC3, activating signal cointegrator 3; CAND1, Cullin-associated and neddylation dissociated 1; HA, hemagglutinin; mRNA, messenger RNA; STAT3, signal transducer and activator of transcription.

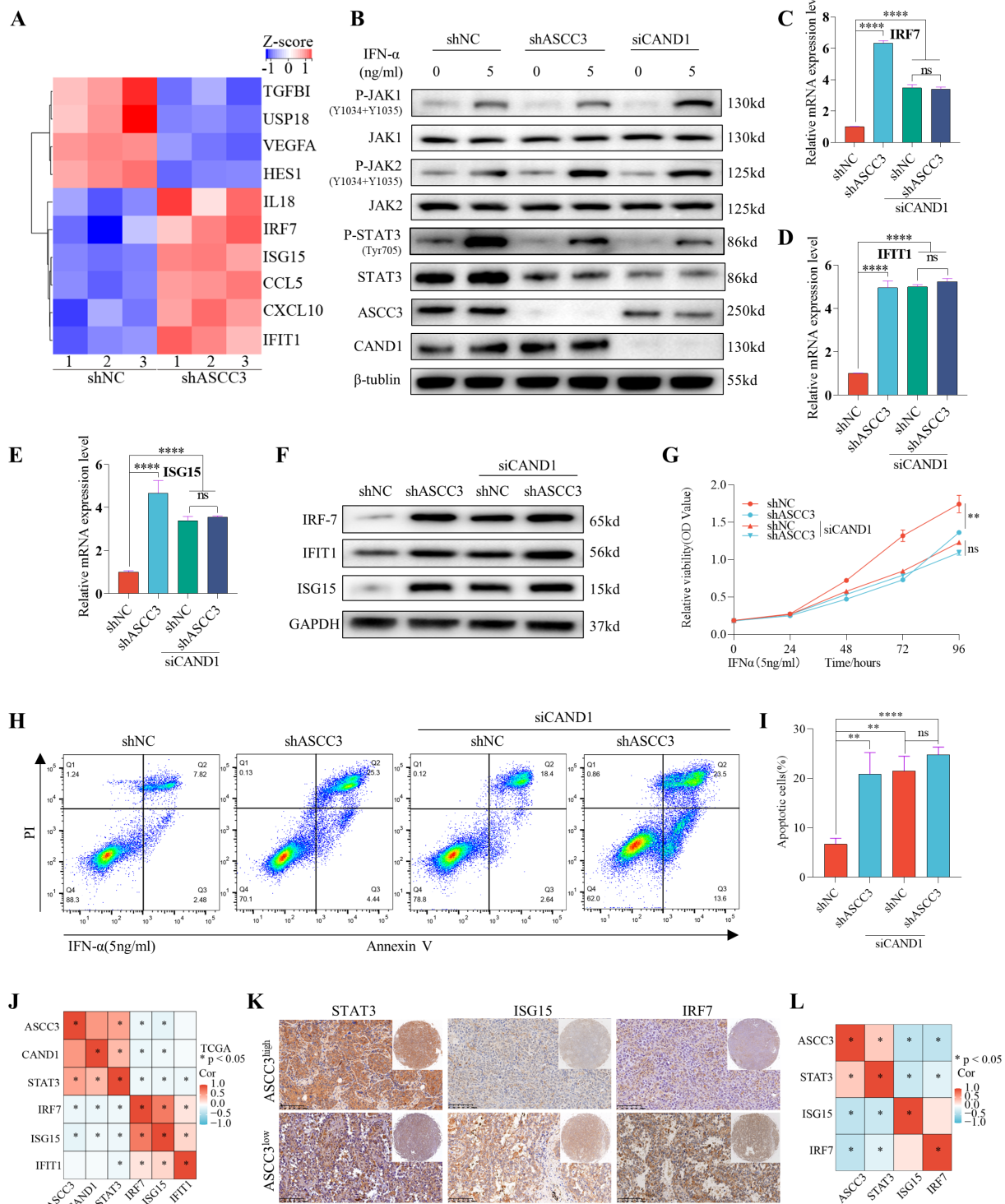


Figure 6 ASCC3 stabilizes STAT3 signaling to inhibit the type I IFN response. (A) RNA sequencing data revealed that type I interferon-stimulated genes were significantly upregulated in H1299-shASCC3 cells, while genes negatively regulating type I interferon signaling were downregulated. (B) Stimulation with IFN- α activated JAK1/2 and STAT3 signaling. (C–F) The knockdown of ASCC3 or interference of CAND1 led to the upregulation of IFN- α -stimulated genes such as IRF7, IFIT1 and ISG15 at both the transcriptional and translational levels. (G–I) The proliferation of H1299-shASCC3 cells was significantly impaired, while apoptosis was markedly enhanced compared with that of the shNC group after stimulation with IFN- α . (J–L) The expression of STAT3 was positively correlated with ASCC3, while the expression of IFN- α -stimulated genes such as IRF7 and ISG15 was negatively correlated with ASCC3 expression (data from TCGA and immunohistochemistry staining of tissue microarray). * $p < 0.05$, ** $p < 0.01$, *** $p < 0.001$, **** $p < 0.0001$, ns: not significant. JAK, Janus Kinase; ASCC3, activating signal cointegrator 3; CAND1, Cullin-associated and neddylation dissociated 1; IFN, interferon; mRNA, messenger RNA; NSCLC, non-small cell lung cancer; pSTAT3, phosphorylated STAT3; STAT3, signal transducer and activator of transcription. PI, propidium iodide; TCGA, The Cancer Genome Atlas.

intraperitoneally (i.p.) at a dose of 100 µg/injection every 3 days when the tumor size reached

100 mm³ (figure 7A). The results showed that knockdown of ASCC3 significantly potentiated the efficacy of anti-PD-1 treatment, as evidenced by the smaller tumor volume and higher inhibition rate in the shASCC3 group than in the shNC group (figure 7B–D). In addition, knockdown of ASCC3 combined with anti-PD-1 therapy substantially improved the survival of mice implanted with subcutaneous tumors (figure 7E). Furthermore, the IHC staining revealed increased proportions of CD8⁺ T cells, NK cells and DCs but a decreased proportion of Tregs from the LLC-shNC+IgG group to the LLC-shASCC3+IgG group and from the LLC-shNC+anti-PD-1 group to the LLC-shASCC3+anti-PD-1 group (figure 7F and online supplemental figure 5). To further explore the expression of ASCC3 and the efficacy of anti-PD-1 therapy, we analyzed the expression pattern and immune profile of NSCLC tissues from 17 patients who received anti-PD-1 therapy. According to the Response Evaluation Criteria in Solid Tumors Version 1.1 (RECIST V.1.1) standard, progressive disease (PD) was observed in eight patients, six patients achieved stable disease (SD), and three patients achieved partial remission (PR). IHC analysis showed that the expression of ASCC3 was significantly higher in the PD group than in the SD and PR groups (figure 7G,H). In addition, the infiltration of CD8⁺ T cells, NK cells and DCs in the PR and SD groups was significantly higher than that in the PD group, while the infiltration of Tregs was higher in the PD group (figure 7I,J). Spearman's analysis demonstrated a positive correlation between the expression of ASCC3 and the infiltration of Tregs but a negative correlation with the infiltration of CD8⁺ T cells, DCs and NK cells in 17 patients with NSCLC who received anti-PD-1 therapy (figure 7K). In conclusion, these findings indicated that inhibition of ASCC3 could improve the efficacy of anti-PD-1 therapy in patients with NSCLC.

Figure 8 summarizes the main findings of this study. ASCC3 overexpression in NSCLC contributes to the immunosuppressive TME and confers resistance to immunotherapy. Mechanistically, ASCC3 recruits CAND1 to stabilize STAT3 signaling by inhibiting the Ub-mediated degradation of STAT3, thereby impairing the type I IFN response in tumor cells and promoting resistance to anti-tumor immune cells. Furthermore, knockdown of ASCC3 combined with anti-PD-1 therapy significantly enhances the susceptibility and efficacy of immunotherapy in patients with NSCLC with high ASCC3 expression.

DISCUSSION

The prognosis of patients with advanced NSCLC remains unsatisfactory. Tumor immune evasion was reported to be associated with early NSCLC metastasis and poor response to immunotherapy.^{36,37} In this research, through analysis of gene expression profiles and IHC staining, we found that ASCC3 was significantly upregulated in NSCLC tissues compared with matched peritumor

tissues, and an even higher expression level was observed in metastatic foci than in primary tumors. High ASCC3 expression was strongly correlated with tumor immunosuppression and poor prognosis in patients with NSCLC. In vitro and in vivo experiments showed that knockdown of ASCC3 resulted in impaired proliferation and invasion of tumor cells and a better response to anti-PD-1 therapy. Mechanistically, we demonstrated that ASCC3 stabilized STAT3 signaling via CAND1 and impaired the type I IFN response, which played an important role in reshaping the TME and promoting the progression of NSCLC.

ASCC3 is primarily located in the cytoplasm, with a smaller portion found in the nucleus, and is known for its helicase activity,¹⁰ which has previously been reported to be associated with DNA damage repair, translation regulation and antiviral immune response.^{14,38–40} For example, ASCC3 was confirmed to promote DNA unwinding to generate a single-stranded substrate, enabling AlkB homolog 3-mediated DNA repair.¹⁴ In addition, ASCC3 is involved in activation of the ribosome quality control pathway that degrades nascent peptide chains during problematic translation.^{38,39} In addition to helicase activity, ASCC3 was reported to play a role as a scaffold to interact with other proteins^{15,29} or recruit other transcriptional or epigenetic regulators to functional sites.^{14,31} Moreover, ASCC3 was reported to be involved in the progression of several solid tumors, such as colorectal cancer and thyroid cancer,^{8,9} affecting immune cell infiltration in the TME and patient prognosis. In a study by Li J *et al*,¹⁰ ASCC3 was identified as a negative regulator of the host immune response. Knockdown of ASCC3 led to the upregulation of multiple antiviral IFN-stimulated genes, which was correlated with the inhibition of virus infection.¹⁰ However, the mechanisms remain largely underexplored, and there is currently no research on the role and mechanisms of ASCC3 in tumors. In this study, we elucidated the role of ASCC3 as a scaffold in recruiting CAND1 and mediating its interaction with STAT3, thereby inhibiting the Ub-mediated degradation of STAT3 and stabilizing JAK/STAT3 signaling, ultimately promoting the progression of NSCLC.

CAND1 is a HEAT repeat-containing protein that inhibits the assembly of multisubunit E3 Ub ligase complexes, generally suppressing Skp1-Cullins-F-box Ub ligase activity and decreasing the Ub-mediated degradation of substrates.^{41,42} CAND1 is highly expressed in many solid tumors and correlated with tumor aggressiveness and progression.^{43–46} For example, CAND1 was reported to bind to nuclear factor-erythroid factor 2-related factor 2 and prevent its ubiquitination and degradation to promote gastric tumorigenesis.⁴⁵ Additionally, CAND1 was upregulated in NSCLC, and miR-33a could inhibit cancer cell proliferation and invasion by targeting CAND1.⁴⁶ In this research, we found that CAND1 had similar biological characteristics to ASCC3 in NSCLC. For instance, CAND1 was upregulated in NSCLC, especially in metastatic foci, and was correlated with poor prognosis in patients with NSCLC. In vitro experiments also revealed

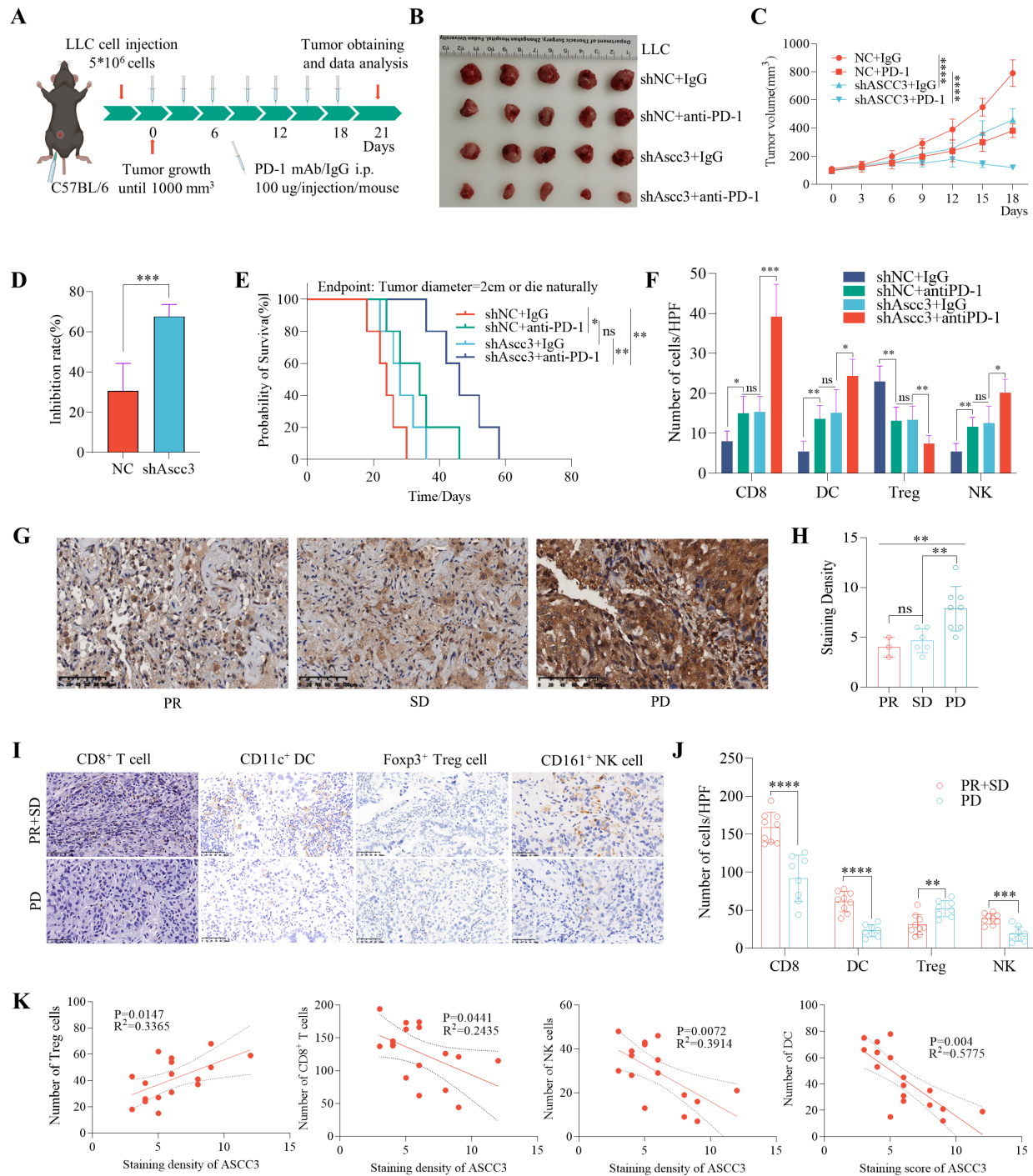


Figure 7 ASCC3 impairs the efficacy of PD-1 blockade, while knockdown of ASCC3 sensitizes NSCLC to anti-PD-1 treatment. (A) The anti-PD-1 antibody or IgG was administered i.p. at a dose of 100 $\mu\text{g}/\text{injection}$ every 3 days when the tumor size reached 100 mm^3 . (B–D) Overexpression of ASCC3 significantly minimized the efficacy of anti-PD-1 treatment, manifesting as a smaller tumor volume and higher inhibition rate in the shASCC3 group than in the shNC group. (E) The knockdown of ASCC3 combined with anti-PD-1 therapy greatly improved the survival of mice implanted with subcutaneous tumors. (F) IHC staining revealed increased proportions of CD8⁺ T cells, NK cells and DCs but a lower proportion of Tregs in the LLC-shNC+IgG group than in the LLC-shASCC3+IgG group and in the LLC-shNC+anti-PD-1 group than in the LLC-shASCC3+anti-PD-1 group. (G,H) IHC analysis showed that the expression of ASCC3 was significantly higher in the PD group than in the SD and PR groups. (I,J) The infiltration of CD8⁺ T cells, NK cells and DCs in the PR and SD groups was significantly higher than that in the PD group, while the infiltration of Tregs was higher in the PD group. (K) The expression of ASCC3 was positively correlated with the infiltration of Tregs but negatively correlated with the infiltration of CD8⁺ T cells, DCs and NK cells in 17 patients with NSCLC who received anti-PD-1 therapy. PD, progressive disease; SD, stable disease; PR, partial remission; * $p < 0.05$, ** $p < 0.01$, *** $p < 0.001$, **** $p < 0.0001$, ns: not significant. PD-1, Programmed death-1; mAb, monoclonal antibody; i.p., intraperitoneal; HPF, high power field; ASCC3, activating signal cointegrator 3; DCs, dendritic cells; Treg, regulatory T cells; IHC, immunohistochemistry; LLC, Lewis lung carcinoma; NK, natural killer; NSCLC, non-small cell lung cancer.

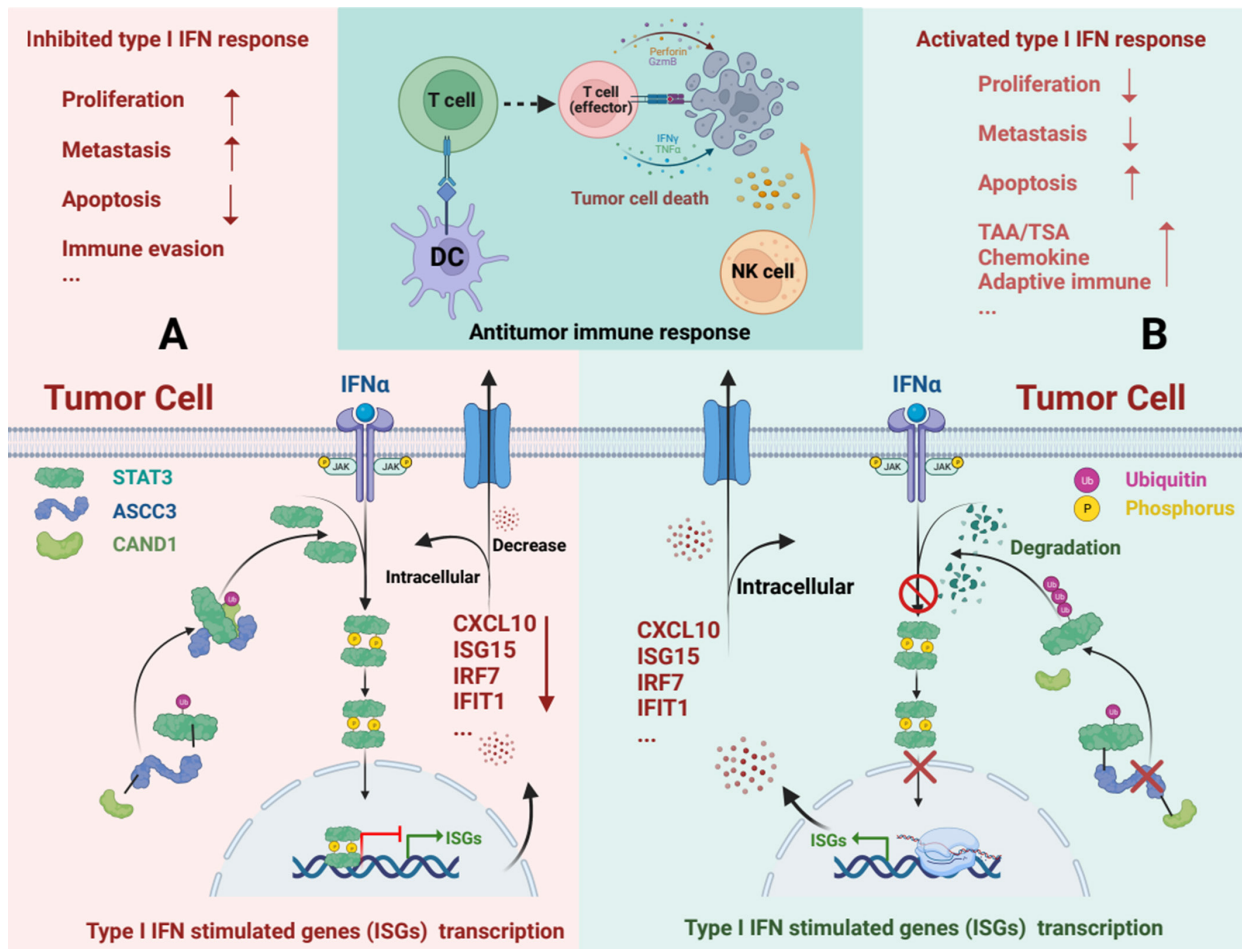


Figure 8 Schematic diagram of the primary findings in this study. (A) Overexpression of ASCC3 recruits CAND1 to inhibit the ubiquitin-mediated degradation of STAT3. Then, phosphorylated STAT3 levels increase and impair the type I IFN response of tumor cells, which downregulates the expression of IFN-activated genes (such as CXCL10, ISG15, IRF7 and IFIT1) and inhibits the antitumor immune response. (B) Knockdown of ASCC3 impairs STAT3 signaling and activates the type I IFN response, which enhances antitumor immune cell function and increases the susceptibility and efficacy of immunotherapy in patients with non-small cell lung cancer with high ASCC3 expression. ASCC3, activating signal cointegrator 3; CAND1, Cullin-associated and neddylation dissociated 1; IFN, interferon; STAT3, signal transducer and activator of transcription; TAA, tumor-associated antigen; TSA, tumor-specific antigen.

the role of CAND1 in tumor promotion. RNA sequencing data analysis showed a potential relationship between ASCC3 and STAT3 signaling, and MS combined with a Co-IP assay revealed the interactions among ASCC3, STAT3 and CAND1. Further exploration confirmed that ASCC3 stabilized STAT3 signaling via CAND1 to reshape the TME of NSCLC.

STAT3 is hyperactivated in the majority of human cancers and is involved in numerous cellular processes, including cell proliferation, angiogenesis, tumor invasion and metastasis, which are generally associated with poor clinical prognosis.⁴⁷ In addition, accumulating evidence has revealed that hyperactivation of STAT3 can mediate tumor-induced immunosuppression at many levels,^{32 33 48} promoting the progression of cancer and mediating therapeutic resistance, particularly cancer immunotherapy. For example, STAT3 can suppress the expression of immune-stimulating factors such as IFNs, proinflammatory cytokines and chemokines.⁴⁸ Interestingly, IFNs can

activate STAT3 signaling; however, STAT3 inhibits the secretion of type I IFNs (IFN-Is) and IFN-I-responsive genes via multiple biological processes, including attenuating IFN-I signaling activation and impairing ISGF3 expression and transactivation.^{49 50} Previous studies have shown the effects of IFN-Is on the host antiviral immune response and their potential role in tumor immunosurveillance and antitumor therapy.^{51 52} Moreover, the efficacy of comprehensive therapy, including immunotherapy, greatly relies on the activation of the IFN-I response.^{53 54} In this investigation, ASCC3 overexpression hindered the type I IFN response, resulting in a reduction in the effectiveness of anti-PD-1 therapy in NSCLC. Thus, we reported that ASCC3 induced immunosuppression via the ASCC3-CAND1/STAT3 axis, which inhibited the IFN-I response in tumor cells and enhanced resistance to the cytotoxic effects of T cells. Interestingly, although we observed that ASCC3 only regulates the expression of STAT3 at the protein level in tumor cells, the bulk

sequencing data from the TCGA database showed a positive correlation between the expression of STAT3 and ASCC3. This might be due to the inclusion of non-tumor cell information. ASCC3 is expressed not only in tumor cells but also in non-tumor cells, particularly immune cells.¹⁰ Therefore, it might also be worthwhile to explore the expression and function of ASCC3 in other cells.

The development of anti-PD-1 and anti-PD-L1 therapies has led to unprecedented prolonged survival for a proportion of patients with advanced tumors, especially metastatic NSCLC.⁵⁵ Inhibiting the PD-1/PD-L1 axis restores the functional state of cytotoxic T cells and augments the immune response against tumors. However, a considerable proportion of patients cannot benefit from such immunotherapy, which is mainly attributed to the complex immunologic regulatory network.⁵⁶ For instance, some cytotoxic T cells enter an irreversible dysfunctional state via other immunoregulatory pathways and cannot be rescued by PD-1/PD-L1 blockade.⁵⁷ Therefore, other immune escape mechanisms within or outside the PD-1/PD-L1 network need to be revealed and targeted to increase the response rate.⁵⁶ Defective gene regulation or gene alteration often affects oncogenic networks, tumor immunogenicity and immune cells involved in antitumor responses.⁵⁸ Our research revealed that high ASCC3 expression impaired the IFN- γ response and induced an immunosuppressive TME, which reduced the effectiveness of anti-PD-1 therapy. We investigated the potential of anti-PD-1 therapy combined with silencing ASCC3, and the preclinical results indicated significantly improved efficacy of anti-PD-1 therapy.

There are several limitations of this research. First, the lack of immune cell expression profiles in the analyzed single-cell sequencing data prevented us from investigating the crosstalk and relationship between different types of immune cells and tumor cells with high ASCC3 expression at the single-cell level. Second, additional research is necessary to elucidate whether ASCC3, STAT3, and CAND1 operate as a functional complex, contributing to tumor progression and metastasis. Additionally, whether the binding of ASCC3 with STAT3 influences ASCC3's binding activity with CAND1 needs further investigation. Third, the lack of small molecule inhibitors targeting ASCC3 hinders the exploration of its combined therapeutic efficacy *in vivo*.

In conclusion, this research revealed a critical role of ASCC3 in reshaping the TME and promoting the progression of NSCLC, and we provided a new molecule that can be targeted to improve the efficacy of anti-PD-1 therapy and the prognosis of patients with NSCLC.

Author affiliations

¹Department of Thoracic Surgery, Zhongshan Hospital, Fudan University, Shanghai, Shanghai, China

²Cancer Center, Zhongshan Hospital, Fudan University, Shanghai, Shanghai, China

³Department of Thoracic Surgery, Changhai Hospital, Naval Medical University, Shanghai, China

⁴School of Basic Medical Sciences, Fudan University, Shanghai, China

⁵Institute of Vascular Disease, Shanghai TCM-Integrated Hospital, Shanghai University of Traditional Chinese Medicine, Shanghai, China

⁶CAS Key Laboratory of Molecular Virology and Immunology, Shanghai Institute of Immunology and Infection, Chinese Academy of Sciences, Beijing, China

Correction notice This article has been corrected since it was first published. Labels have been added to figure 5J to clarify the group information for each immunoblot band.

Acknowledgements We thank AJE for English language editing. This manuscript was edited for the English language by AJE. We also thank BioRender because we created the schematic diagram by BioRender.com.

Contributors Y-QA and JG performed the experiments and acquired data. Y-QA, JG, JC and SW contributed to the data analysis and wrote the manuscript. L-CZ and JD revised the figures and supplemental materials. Z-WC and H-KW supervised statistical analyses and contributed to the methodology. H-KW, J-HJ and J-YD provided guidance of experimental design and necessary fundings. All authors supervised and confirmed the manuscript. J-HJ and J-YD are responsible for the overall content as the guarantors with full responsibility for the work and/or the conduct of the study, capability of accessing the data, and controlling the decision to publish.

Funding This research was funded by grants from the National Natural Science Foundation of China (81972168), Strategic Priority Research Program of the Chinese Academy of Sciences (XDB29030103) and National Key R&D Program of China (2021YFA1301402).

Competing interests None declared.

Patient consent for publication Not applicable.

Ethics approval This study involves human participants and was approved by Ethics Committee of the Zhongshan Hospital Biomedical Research Department, Zhongshan Hospital, Fudan University (approval number Y2019-187). Participants gave informed consent to participate in the study before taking part.

Provenance and peer review Not commissioned; externally peer reviewed.

Data availability statement No data are available. All data generated that are relevant to the results presented in this article are included in this article and the supplemental materials. Other data that are not relevant for the results presented here are available from the corresponding author J-YD upon reasonable request.

Supplemental material This content has been supplied by the author(s). It has not been vetted by BMJ Publishing Group Limited (BMJ) and may not have been peer-reviewed. Any opinions or recommendations discussed are solely those of the author(s) and are not endorsed by BMJ. BMJ disclaims all liability and responsibility arising from any reliance placed on the content. Where the content includes any translated material, BMJ does not warrant the accuracy and reliability of the translations (including but not limited to local regulations, clinical guidelines, terminology, drug names and drug dosages), and is not responsible for any error and/or omissions arising from translation and adaptation or otherwise.

Open access This is an open access article distributed in accordance with the Creative Commons Attribution Non Commercial (CC BY-NC 4.0) license, which permits others to distribute, remix, adapt, build upon this work non-commercially, and license their derivative works on different terms, provided the original work is properly cited, appropriate credit is given, any changes made indicated, and the use is non-commercial. See <http://creativecommons.org/licenses/by-nc/4.0/>.

ORCID iD

Jian-Yong Ding <http://orcid.org/0000-0003-2729-3141>

REFERENCES

- Sung H, Ferlay J, Siegel RL, *et al.* Global Cancer Statistics 2020: GLOBOCAN estimates of incidence and mortality worldwide for 36 cancers in 185 countries. *CA Cancer J Clin* 2021;71:209–49.
- Herbst RS, Morgensztern D, Boshoff C. The biology and management of non-small cell lung cancer. *Nature* 2018;553:446–54.
- Weir BA, Woo MS, Getz G, *et al.* Characterizing the cancer genome in lung adenocarcinoma. *Nature* 2007;450:893–8.
- Sequist LV, Yang JC-H, Yamamoto N, *et al.* Phase III study of Afatinib or cisplatin plus pemetrexed in patients with metastatic lung adenocarcinoma with EGFR mutations. *J Clin Oncol* 2013;31:3327–34.

- 5 Peters S, Camidge DR, Shaw AT, *et al.* Alectinib versus Crizotinib in untreated ALK-positive non-small-cell lung cancer. *N Engl J Med* 2017;377:829–38.
- 6 Adderley H, Blackhall FH, Lindsay CR. KRAS-mutant non-small cell lung cancer: converging small molecules and immune checkpoint inhibition. *EBioMedicine* 2019;41:711–6.
- 7 Hirsch FR, Scagliotti GV, Mulshine JL, *et al.* Lung cancer: current therapies and new targeted treatments. *Lancet* 2017;389:299–311.
- 8 Jia M, Li Z, Pan M, *et al.* Evaluation of immune infiltrating of thyroid cancer based on the intrinsic correlation between pair-wise immune genes. *Life Sci* 2020;259:118248.
- 9 Frank B, Burwinkel B, Bermejo JL, *et al.* Ten recently identified associations between nsSNPs and colorectal cancer could not be replicated in German families. *Cancer Lett* 2008;271:153–7.
- 10 Li J, Ding SC, Cho H, *et al.* A short hairpin RNA screen of interferon-stimulated genes identifies a novel negative regulator of the cellular antiviral response. *mBio* 2013;4:e00385–13.
- 11 Zhang Z, Cui F, Zhou M, *et al.* Single-cell RNA sequencing analysis identifies key genes in brain metastasis from lung adenocarcinoma. *Curr Gene Ther* 2021;21:338–48.
- 12 Kim N, Kim HK, Lee K, *et al.* Single-cell RNA sequencing demonstrates the molecular and cellular reprogramming of metastatic lung adenocarcinoma. *Nat Commun* 2020;11:2285.
- 13 Gao Y, Li G, Sun L, *et al.* ACTN4 and the pathways associated with cell motility and adhesion contribute to the process of lung cancer metastasis to the brain. *BMC Cancer* 2015;15:277.
- 14 Dango S, Mosammamparast N, Sowa ME, *et al.* DNA unwinding by ASCC3 helicase is coupled to ALKBH3-dependent DNA alkylation repair and cancer cell proliferation. *Mol Cell* 2011;44:373–84.
- 15 Brickner JR, Soll JM, Lombardi PM, *et al.* A ubiquitin-dependent signalling axis specific for ALKBH-mediated DNA dealkylation repair. *Nature* 2017;551:389–93.
- 16 Yu H, Lee H, Herrmann A, *et al.* Revisiting STAT3 signalling in cancer: new and unexpected biological functions. *Nat Rev Cancer* 2014;14:736–46.
- 17 Hillmer EJ, Zhang H, Li HS, *et al.* STAT3 signaling in immunity. *Cytokine & Growth Factor Reviews* 2016;31:1–15.
- 18 Sgrignani J, Garofalo M, Matkovic M, *et al.* Structural biology of STAT3 and its implications for anticancer therapies development. *Int J Mol Sci* 2018;19:1591.
- 19 Zou S, Tong Q, Liu B, *et al.* Targeting STAT3 in cancer immunotherapy. *Mol Cancer* 2020;19:145.
- 20 Wei C-Y, Zhu M-X, Yang Y-W, *et al.* Downregulation of RNF128 activates WNT/β-Catenin signaling to induce cellular EMT and stemness via CD44 and CTTN ubiquitination in melanoma. *J Hematol Oncol* 2019;12:21.
- 21 Ke A-W, Shi G-M, Zhou J, *et al.* CD151 amplifies signaling by integrin α6β1 to PI3K and induces the epithelial-mesenchymal transition in HCC cells. *Gastroenterology* 2011;140:1629–41.
- 22 Huang X-Y, Ke A-W, Shi G-M, *et al.* αB-crystallin complexes with 14-3-3Z to induce epithelial-mesenchymal transition and resistance to sorafenib in hepatocellular carcinoma. *Hepatology* 2013;57:2235–47.
- 23 Zhang L-X, Gao J, Long X, *et al.* The circular RNA circHMGB2 drives immunosuppression and anti-PD-1 resistance in lung adenocarcinomas and squamous cell carcinomas via the miR-181A-5P/CARM1 axis. *Mol Cancer* 2022;21:110.
- 24 Cai J, Shi G, Dong Z, *et al.* Ubiquitin-specific protease 7 accelerates P14(ARF) degradation by deubiquitinating thyroid hormone receptor-interacting protein 12 and promotes hepatocellular carcinoma progression. *Hepatology* 2015;61:1603–14.
- 25 Gao A, Sun T, Ma G, *et al.* LEM4 confers tamoxifen resistance to breast cancer cells by activating cyclin D-CDK4/6-Rb and ERα pathway. *Nat Commun* 2018;9:4180.
- 26 Geng J, Yu S, Zhao H, *et al.* The transcriptional coactivator TAZ regulates reciprocal differentiation of T(H)17 cells and T(reg) cells. *Nat Immunol* 2017;18:800–12.
- 27 Sáenz JB, Vargas N, Mills JC. Tropism for spasmodic polypeptide-expressing metaplasia allows helicobacter pylori to expand its intragastric niche. *Gastroenterology* 2019;156:160–74.
- 28 Juskiewicz S, Speldewinde SH, Wan L, *et al.* The ASC-1 complex disassembles collided ribosomes. *Mol Cell* 2020;79:603–14.
- 29 Soll JM, Brickner JR, Mudge MC, *et al.* RNA ligase-like domain in activating signal cointegrator 1 complex subunit 1 (ASCC1) regulates ASCC complex function during alkylation damage. *Journal of Biological Chemistry* 2018;293:13524–33.
- 30 Wollen KL, Hagen L, Vågbo CB, *et al.* ALKBH3 partner ASCC3 mediates P-body formation and selective clearance of MMS-induced 1-methyladenosine and 3-methylcytosine from mRNA. *J Transl Med* 2021;19:287.
- 31 Jung D-J, Sung H-S, Goo Y-W, *et al.* Novel transcription coactivator complex containing activating signal cointegrator 1. *Mol Cell Biol* 2002;22:5203–11.
- 32 Villarino AV, Kanno Y, O’Shea JJ. Mechanisms and consequences of JAK-STAT signaling in the immune system. *Nat Immunol* 2017;18:374–84.
- 33 Kortylewski M, Kujawski M, Wang T, *et al.* Inhibiting STAT3 signaling in the hematopoietic system elicits multicomponent antitumor immunity. *Nat Med* 2005;11:1314–21.
- 34 Hu B, Yu M, Ma X, *et al.* IFNα potentiates anti-PD-1 efficacy by remodeling glucose metabolism in the hepatocellular carcinoma microenvironment. *Cancer Discov* 2022;12:1718–41.
- 35 Zhu Y, Chen M, Xu D, *et al.* The combination of PD-1 blockade with interferon-α has a synergistic effect on hepatocellular carcinoma. *Cell Mol Immunol* 2022;19:726–37.
- 36 Maimon A, Levi-Yahid V, Ben-Meir K, *et al.* Myeloid cell-derived PROS1 inhibits tumor metastasis by regulating inflammatory and immune responses via IL-10. *J Clin Invest* 2021;131:e126089.
- 37 Mascaux C, Angelova M, Vasaturo A, *et al.* Immune evasion before tumour invasion in early lung squamous carcinogenesis. *Nature* 2019;571:570–5.
- 38 Matsuo Y, Ikeuchi K, Saeki Y, *et al.* Ubiquitination of stalled ribosome triggers ribosome-associated quality control. *Nat Commun* 2017;8:159.
- 39 Hashimoto S, Sugiyama T, Yamazaki R, *et al.* Identification of a novel trigger complex that facilitates ribosome-associated quality control in mammalian cells. *Sci Rep* 2020;10:3422.
- 40 Pinto R, Vågbo CB, Jakobsson ME, *et al.* The human methyltransferase ZCCHC4 catalyses N6-methyladenosine modification of 28S Ribosomal RNA. *Nucleic Acids Res* 2020;48:830–46.
- 41 Liu X, Reitsma JM, Mamrosch JL, *et al.* Cand1-mediated adaptive exchange mechanism enables variation in F-box protein expression. *Mol Cell* 2018;69:773–86.
- 42 Liu J, Furukawa M, Matsumoto T, *et al.* NEDD8 modification of CUL1 Dissociates P120(CAND1), an inhibitor of CUL1-SKP1 binding and SCF ligases. *Mol Cell* 2002;10:1511–8.
- 43 Korzeniewski N, Hohenfellner M, Duensing S. CAND1 promotes PLK4-mediated centriole overduplication and is frequently disrupted in prostate cancer. *Neoplasia* 2012;14:799–806.
- 44 Eigentler A, Tymozuk P, Zwick J, *et al.* The impact of CAND1 in prostate cancer. *Cancers (Basel)* 2020;12:428.
- 45 Chen T, Jinlin D, Wang F, *et al.* GSTM3 deficiency Impedes DNA mismatch repair to promote gastric tumorigenesis via CAND1/NRF2-KEAP1 signaling. *Cancer Lett* 2022;538:215692.
- 46 Kang M, Li Y, Zhao Y, *et al.* miR-33A inhibits cell proliferation and invasion by targeting CAND1 in lung cancer. *Clin Transl Oncol* 2018;20:457–66.
- 47 Johnson DE, O’Keefe RA, Grandis JR. Targeting the IL-6/JAK/STAT3 signalling axis in cancer. *Nat Rev Clin Oncol* 2018;15:234–48.
- 48 Wang T, Niu G, Kortylewski M, *et al.* Regulation of the innate and adaptive immune responses by STAT-3 signaling in tumor cells. *Nat Med* 2004;10:48–54.
- 49 Icardi L, Lievens S, Mori R, *et al.* Opposed regulation of type I IFN-induced STAT3 and ISGF3 transcriptional activities by histone deacetylases (HDACS) 1 and 2. *FASEB J* 2012;26:240–9.
- 50 Tsai MH, Pai LM, Lee CK. Fine-tuning of type I interferon response by STAT3. *Front Immunol* 2019;10:1448.
- 51 Snell LM, McGaha TL, Brooks DG. Type I interferon in chronic virus infection and cancer. *Trends Immunol* 2017;38:542–57.
- 52 Yu R, Zhu B, Chen D. Type I interferon-mediated tumor immunity and its role in immunotherapy. *Cell Mol Life Sci* 2022;79:191.
- 53 Zitvogel L, Galluzzi L, Kepp O, *et al.* Type I interferons in anticancer immunity. *Nat Rev Immunol* 2015;15:405–14.
- 54 Chen L, Musa AE. Boosting immune system against cancer by resveratrol. *Phytotherapy Research* 2021;35:5514–26.
- 55 Reck M, Remon J, Hellmann MD. First-line immunotherapy for non-small-cell lung cancer. *J Clin Oncol* 2022;40:586–97.
- 56 Xu-Monette ZY, Zhang M, Li J, *et al.* PD-1/PD-L1 blockade: have we found the key to unleash the antitumor immune response *Front Immunol* 2017;8:1597.
- 57 Schietinger A, Philip M, Krisnawan VE, *et al.* Tumor-specific T cell dysfunction is a dynamic antigen-driven differentiation program initiated early during tumorigenesis. *Immunity* 2016;45:389–401.
- 58 Hogg SJ, Beavis PA, Dawson MA, *et al.* Targeting the epigenetic regulation of antitumour immunity. *Nat Rev Drug Discov* 2020;19:776–800.